Proc. of the 5th WSEAS/IASME Int. Conf. on Electric Power Systems, High Voltages, Electric Machines, Tenerife, Spain, December 16-18, 2005 (pp392-397)

Swift Periodic Steady State Solution of Distribution Systems Containing DVRs

A. Medina[1], Edgar O. Hernández-Martínez[2], D. Olguín-Salinas[3]

[1] Facultad de Ingeniería Eléctrica, División de Estudios de Posgrado, U.M.S.N.H., Ciudad Universitaria, C.P. 58030, Morelia, Michoacán, MEXICO
[2] Instituto de Investigaciones Eléctricas, División de Sistemas Eléctricos, Gerencia de Uso de Energía Eléctrica, Edificio 12, 2º Piso, Calle Reforma No. 113 Col. Palmira, C.P. 62490, Cuernavaca, Morelos, MEXICO
[3] Instituto Politécnico Nacional, ESIME, Sección de Estudios de Posgrado e Investigación, Departamento de Ingeniería Eléctrica, Unidad Profesional "Adolfo López Mateos", Edificio Z-4, 1er piso, Col Lindavista, C.P. 07738, MEXICO D.F.
http://faraday.fie.umich.mx, http://www.iie.org.mx

Abstract: - This contribution details a state space model for a Custom Power component, the Dynamic Voltage Restorer (DVR), for steady state analysis. An efficient time domain methodology is applied which allows a swift computation of the periodic steady state solution for the DVR and the entire distribution network by extrapolating the solution to the limit cycle and thus to the steady state. This is achieved with the application of a Newton technique based on a Numerical differentiation (ND) procedure. Comparisons are shown in terms of computer efficiency against the conventional Brute Force (BF) solution obtained using the Fourth-Order Runge-Kutta numerical integration method.

Key-Words: - Custom Power, Dynamic Voltage Restorer, steady state, time domain, limit cycle, Newton technique, Numerical Differentiation, Runge-Kutta.

1 Introduction

At present, voltage depressions or sags are considered the dominant disturbances affecting power quality in distribution systems [1]. It is understood that a voltage sag is not as damaging to industry as along or short interruption. However, there are far more voltage sags than interruptions the total damage due to sags is still larger. Short interruptions and long interruptions originate in the local distribution network. However, voltage sags at equipment terminals can be due to short-circuit faults hundreds of kilometers away in the transmission systems. A voltage sag is thus much more of a "global" problem than an interruption [2]. The Dynamic Voltage Restorer (DVR), a member of the Custom Power components [3] is at present regarded as the most efficient device available to solve voltage sag problems [1]. This is a power electronics controller which protects sensitive loads against temporary voltage interruptions due to sags/swells generated at the power plant supply [4]. During a voltage depression, the device supplies reactive energy to the distribution system for sag compensation [1]. The DVR has the capability of independently generating of absorbing controllable real and reactive power at its alternating current terminals [4]. The first series dynamic voltage restorer based on inverter technology was installed in 1994. Since then several more have been installed throughout the world. The applications have been on both low-voltage and medium-voltage applications, with load rating from 1 MVA to 6.5 MVA. Examples are the installations by Duke Power, USA, in 1996, Powercor, Ltd, Australia, in 1997 and Scottish Power, Sotland, with 2 MVA and 4 MVA ratings respectively [5]. The DVR has been commissioned for correcting voltage sags/swells in these systems. Fig. 1 illustrates a typical DVR diagram. It can be observed that the DVR injects appropriate phasor voltages in each phase through injection transformers connected in series [6] and in synchronism with the distribution feeders [7].

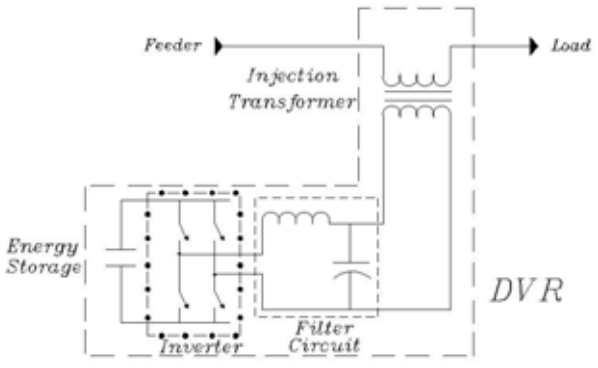

Fig. 1. Typical schematic of a single-phase DVR.

2 State space DVR model

Two different DVR structures have been proposed [4]. In the first one, a capacitive filter is connected at the secondary side of the injection transformer, e.g. at the distribution system side. This prevents switching frequency harmonics from entering the system. The main drawback comes from the fact that the direct connection from the Voltage Source Inverter (VSI) to the injection transformer primary side results in transformer circuit losses, since the flux variations of high frequencies produce important losses increments in the transformer core. To avoid this, a second structure is used were the LC filter is located at the primary side of the injection transformer and the secondary transformer side is directly connected to the distribution feeder, as shown in Fig. 1 [4]. This filtering arrangement is preferred, as it is known that locating the filter closer to the harmonic source results in an adequate strategy for harmonic mitigation [1]. This structure is used in the present contribution.

The DVR operation is based on solid state power electronics inverter commuters with modulating width pulses (PWM) [4]. The VSI syntheses the injection voltages required for sags compensation. The filter at the primary side of the injection transformer attenuates the high order harmonics produced by the inverter commutation, while the injection transformer is used for increasing and coupling to the distribution system the injected voltage [1].

The Fig. 2 illustrates the single phase DVR equivalent circuit with an LC filter at the primary side of the injection transformer. Here the DVR harmonic filter has an inductance L_f and a capacitance C. The inductance L_T represents the leakage inductance of the injection transformer. The VSI commutation losses are represented by the resistance R_i, the VSI pulse width modulation is given by the variable voltage source $v_0 = v_{dc}\ U$ where v_{dc} is the VSI direct current voltage and U is the inverter commutating state. The current source i_s is assumed to be an independent forcing function in the equivalent circuit [4].

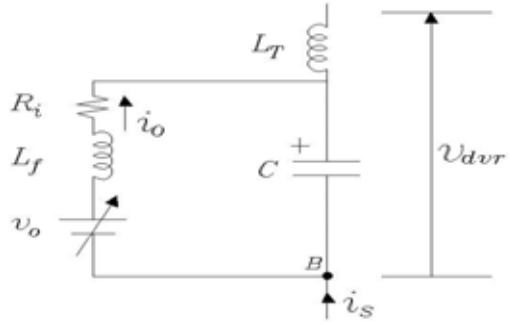

Fig. 2. DVR equivalent circuit with LC filter.

The state space framework allows representing the DVR behavior with a set of differential equations [7]. Defining the state vector $x^T = [i_0 \quad v_c]$, a mathematical model describing the DVR dynamic behavior is obtained from Fig. 2 as,

$$\dot{x} = \begin{bmatrix} -R_i/L_f & -1/L_f \\ 1/C & 0 \end{bmatrix} x + \begin{bmatrix} v_{dc}/L_f & 0 \\ 0 & -1/C \end{bmatrix} \begin{bmatrix} U \\ i_s \end{bmatrix} \quad (1)$$

The supplied or absorbed DVR voltage is,

$$v_{dvr} = v_c - L_T \frac{di_s}{dt} \quad (2)$$

The total voltage delivered to the sensitive load is,

$$v_2 = v_1 + v_{dvr} \quad (3)$$

The corresponding phasor diagram is illustrated in Fig. 3.

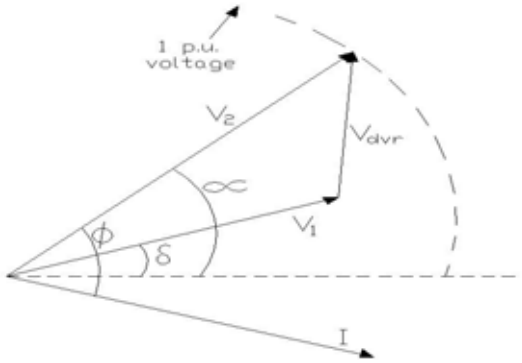

Fig. 3. Phasor diagram describing the DVR operation.

Where V_1, V_2 and V_{dvr} are the magnitudes of the supply voltage, load-side compensated voltage and the DVR injected voltage, respectively. Besides, I, ϕ, δ and α represent the load current, the load power factor, the supply voltage phase angle and the advanced load voltage phase angle, respectively [7].

3 Extrapolation to the limit cycle

The behavior of nonlinear components or loads can be described in the time domain by a set of Ordinary Differential Equations (ODEs) of the form,

$$\dot{x} = f(x,t) \quad (4)$$

where x is a state vector of m elements x_k. If a driving force of period T is assumed, then $f(.,t)$ is a T-periodic vector. The steady state $x(t)$ is in addition periodic and can be represented as x_k in terms of other periodic

element of x or in terms of a T-periodic function [8]. Before reaching the limit cycle [9] the cycles of any transient orbit are relatively close to it, so that a Newton method can be used to extrapolate the solution to the limit cycle. In [8] details are given on the procedure to transform a nonlinear problem (4) into a Newton problem $\Delta x = J(t)\Delta x$ .The extrapolation of the solution to the limit cycle is achieved with the recursive equation [8],

$$x^{\infty} = x^{i} + C\left(x^{i+1} - x^{i}\right) \tag{5}$$

where,

$$C = \left(I - \Phi\right)^{-1} \tag{6}$$

x^{∞} state variables at the limit cycle

x^{i} state variables at the beginning of the base cycle [8]

x^{i+1} state variables at the end of the base cycle

Φ, C, I identification, iteration and unit matrix, respectively.

The solution of (5) implies a quadratic convergence process if Φ and C are updated for each evaluation of x^{∞} and linear for their single or partial iterative evaluation [8]. The matrix Φ is of $n \times n$ order, where n is the number of state variables. Usually $J(t)$ can be analytically obtained, but this is not always the case, in special with highly nonlinear or commutated components. Alternatively Φ can be obtained by columns by the sequential perturbation of state variables $x^{i} + \varepsilon e^{i}$, where ε is a small number, e.g. 10^{-6} and e^{i} is the column i of the unit matrix I. In this investigation a Numerical Differentiation (ND) method [8] was used for this purpose.

4 Test Cases

4.1 System without DVR

The electric network illustrated by Fig. 4 contains two generation sources, represented as sinusoidal functions of 1.0 *p.u.* amplitude, six nodes, six transmission lines represented by simplified R-L branches, three electric arc furnaces, two shunt capacitors connected to nodes 3 and 5 for reactive power compensation, two nonlinear magnetizing branches a TSC connected to node 2 with a switching angle of 120° and a distribution transformer connected to node 3, in parallel with an arc furnace. A convergence criterium of 10^{-10} *p.u.* between successive estimations of x^{∞} is used. Appendix A.1 gives the network parameters used for the test network.

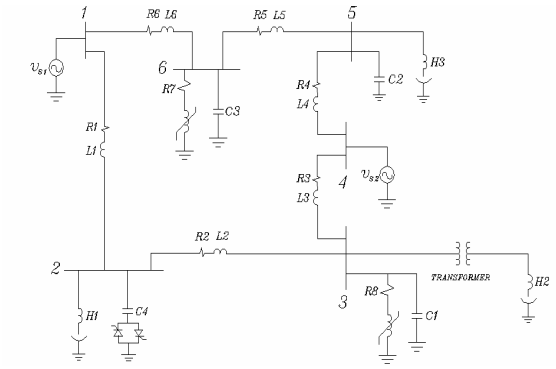

Fig. 4. Test network 1.

The system dynamic behaviour is represented by a set of eighteen ODEs. The Table 1 shows the results obtained for the time domain solution of the test network, given as maximum errors obtained during the BF and ND processes and number of cycles (NC) needed to reach the limit cycle and thus the periodic steady state solution. The conventional BF method required 307 cycles to reach the limit cycle, whereas the ND method needed 84. This represents the 27% of those needed by the BF procedure.

Table 1. Maximum errors during BF and ND solutions

NC	BF	ND
1	3.598301E+00	3.598301E+00
2	1.432803E+00	1.432803E+00
3	2.564709E+00	2.564709E+00
⋮	⋮	⋮
8	1.142138E+00	1.142138E+00
27	2.197498E-01	6.603436E-01
46	5.312626E-02	1.147981E-03
65	1.058870E-02	1.856051E-08
84	3.423970E-03	2.842171E-14
⋮	⋮	
307	9.761014E-11	

The Fig. 5 illustrates the voltage behaviour at the distribution transformer terminals. The 0.8 p.u. waveform represents a significant voltage depression due to the arc furnace operation. The harmonic spectrum is illustrated by Fig. 6 with the third, fifth, seventh, ninth and fifteenth harmonics being of 17, 3, 1, 0.7 and 1.3%, respectively.

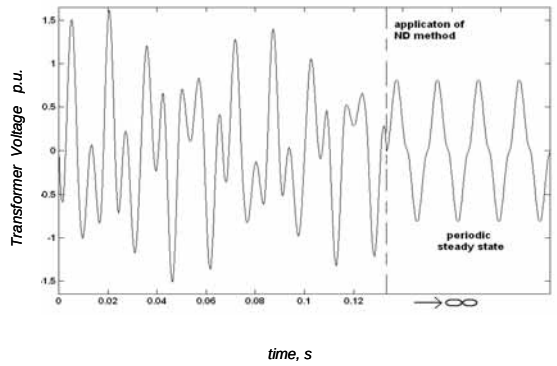

Fig. 5. Time domain voltage in distribution transformer.

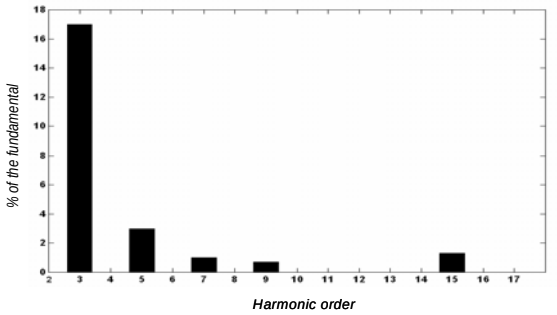

Fig. 6. Voltage harmonics in distribution transformer.

4.2 System with DVR

The test system of Fig. 4 is now solved without a distribution transformer and having a DVR instead, as shown by Fig. 7. This DVR is connected to stand voltage sags caused by the operation of the arc furnace. The system dynamics are represented by a set of twenty ODEs. Appendices A.2 and A.3 give the network parameters and the state space equation, respectively, for the electric system.

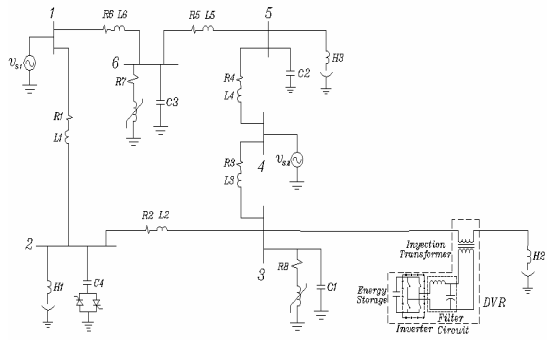

Fig. 7. Test network 2.

Table 2 summarizes the results obtained during the time domain solution process of the analyzed test network, in terms of the number of cycles needed to achieve the limit cycle and thus the steady state solution. It can be noticed that the BF method requires 584 cycles, whereas the ND method 113, corresponding to 19% of those needed by the BF procedure.

Table 2. Maximum errors during FB and ND solutions

NC	BF	ND
1	4.429466E+00	4.429466E+00
2	3.035021E+00	3.035021E+00
3	3.595759E+00	3.595759E+00
⋮	⋮	⋮
8	2.916176E+00	2.916176E+00
29	1.009377E+00	6.025632E-02
50	9.202380E-01	4.434352E-03
71	3.353640E-01	1.514872E-05
92	9.362810E-02	3.065731E-10
113	3.526523E-02	9.103828E-15
⋮	⋮	
584	8.956033E-11	

The time domain solution process is detailed shown by Fig 8. The ND method is applied in t = 0.13 secs. It can be observed that the DVR effectively corrects the voltage depression produced by the electric arc furnace operation. The voltage amplitude is now 1 *p.u.* with the third, fifth, seventh, ninth and fifteenth harmonics being of 3, 0.5, 0.2 and 0.3% respectively, see Fig. 9.

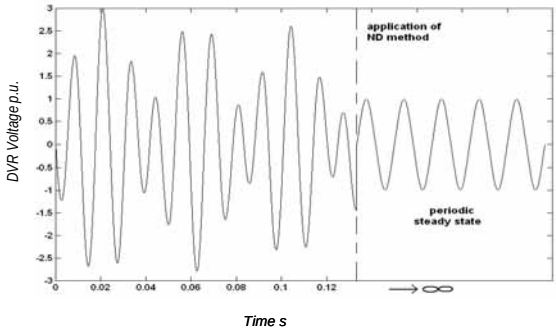

Fig. 8. Evolution of time domain voltage in DVR.

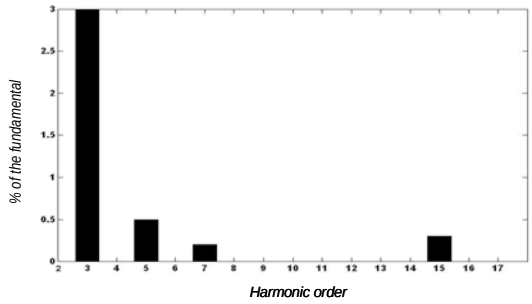

Fig. 9. Voltage harmonics at DVR terminals.

5 Conclusions

A swift steady state solution in the time domain of nonlinear distribution systems containing DVRs for sags/swells voltage compensation has been obtained with the application of a Newton method based on a Numerical Differentiation procedure.

The impact on the system of the DVR for correcting voltage sags due to the electric arc furnace operation

has been illustrated. The time-varying network components, e.g. TSCs, arc furnaces and DVRs have been represented by state space models based on ordinary differential equation sets.

Computer efficiency comparisons have been presented in terms of the numbers of periods (cycles) of time required by the BF and the ND Newton methods, respectively. It can be conclude, from the analyzed cases, that the ND method requires on average 27% of the total numbers of periods of time needed by the BF technique to obtain the steady state solution.

Acknowledgements

The authors want to acknowledge the Universidad Michoacana de San Nicolás de Hidalgo (UMSNH) through the División de Estudios de Posgrado of the Facultad de Ingeniería Eléctrica, the Instituto Politécnico Nacional (ESIME-IPN) and the Instituto de Investigaciones Eléctricas (IIE) for the facilities granted to carry-out this investigation. Edgar Martínez acknowledges financial support and facilities received from IIE to pursue his MSc studies.

References:

[1] S.S. Choi, B.H. Li and D.M. Vilathgamuwa, "Design and Analysis of the Inverter-Side Filter Used in the Dynamic Voltage Restorer", IEEE Transactions on Power Delivery, Vol.17, No.3, July 2002, pp.857-864.
[2] M.H.J. Bollen, "Understanding Power Quality Problems - voltage sags and interruptions", IEEE Press series on Power Engineering, 2000.
[3] N. Hingorani, "Introducing Custom Power", IEEE Spectrum, Vol. 32, No.6, June 1995, pp. 41-48.
[4] A. Ghosh and G. Ledwich, "Structures and Control of a Dynamic Voltage Regulator (DVR)", IEEE Power Engineering Society Winter Meeting, Vol. 3, 2001, pp.1027-1032.
[5] Working Group 14.31 "Custom Power - State of the art", Cigre, August 2002.
[6] T. Jauch, A. Kara, M. Rahmani, D. Westermann "Power Quality Ensured by Dynamic Voltage Correction", Review ABB-4, 1998, pp.25-36.
[7] M. Vilathgamuwa, A.A.D. Ranjith Perera y S.S. Choi, "Performance Improvement of the Dynamic Voltage Restorer With Closed-Loop Load Voltage and Current-Mode Control", IEEE Transactions on Power Electronics, Vol.17, No.5, September 2002, pp. 824-834.
[8] A. Semlyen, A. Medina "Computation of the Periodic Steady State in Systems with Nonlinear Components Using a Hybrid Time and Frequency Domain Methodology", IEEE Transactions on Power Systems, Vol. 10, No.3, August 1995, pp. 1498-1504.
[9] T.S. Parker and L.O. Chua "Practical Numerical Algorithms for Chaotic Systems", Springer-Verlag, NY, 1989.

Appendices

A.1 Test network 1 Parameters

R1=0.01, R2=0.012, R3=0.007, R4=0.018, R5=0.009, R6=0.015, RM1=0.1, RM2=0.1,
L1=0.18, L2=0.11, L3=0.15, L4=0.22, L5=0.19, L6=0.13
LH1=0.14, LH2=0.19, LH3=0.24, LH4=0.21, C1=0.36, C2=0.25, C3=0.31, C4=0.22
km1=0.004, km2=0.0005, km3=0.005

A.2 Test network 2 Parameters

R_I=0.001, L_F=0.15, C_F=0.5, L_T=0.2

A.3 State space equation for the test network 2

$$\dot{X} = Ax + Bu \tag{A.1}$$

$$\dot{X} = \begin{bmatrix} \dot{\psi}_{L1} & \dot{\psi}_{L2} & \dot{\psi}_{L3} & \dot{\psi}_{L4} & \dot{\psi}_{L5} & \dot{\psi}_{L6} & \dot{\psi}_{L7} & \dot{\psi}_{L8} & \dot{\upsilon}_f & \dot{i}_o & \dot{\psi}_{H1} & \dot{\psi}_{H2} & \dot{\psi}_{H3} & \dot{r}_{H1} & \dot{r}_{H2} & \dot{r}_{H3} & \dot{\upsilon}_{C1} & \dot{\upsilon}_{C2} & \dot{\upsilon}_{C3} & \dot{\upsilon}_{C4} \end{bmatrix}^T$$

$$A = \begin{bmatrix}
\frac{-R1}{L1} & 0 & 0 & 0 & 0 & 0 & 0 & 0 & 0 & 0 & 0 & 0 & 0 & 0 & 0 & 0 & 0 & 0 & 0 & -1 \\
0 & \frac{-R2}{L2} & 0 & 0 & 0 & 0 & 0 & 0 & 0 & 0 & 0 & 0 & 0 & 0 & 0 & 0 & -1 & 0 & 0 & 1 \\
0 & 0 & \frac{-R3}{L3} & 0 & 0 & 0 & 0 & 0 & 0 & 0 & 0 & 0 & 0 & 0 & 0 & 0 & -1 & 0 & 0 & 0 \\
0 & 0 & 0 & \frac{-R4}{L4} & 0 & 0 & 0 & 0 & 0 & 0 & 0 & 0 & 0 & 0 & 0 & 0 & 0 & -1 & 0 & 0 \\
0 & 0 & 0 & 0 & \frac{-R5}{L5} & 0 & 0 & 0 & 0 & 0 & 0 & 0 & 0 & 0 & 0 & 0 & 0 & -1 & 1 & 0 \\
0 & 0 & 0 & 0 & 0 & \frac{-R6}{L6} & 0 & 0 & 0 & 0 & 0 & 0 & 0 & 0 & 0 & 0 & 0 & 0 & -1 & 0 \\
0 & 0 & 0 & 0 & 0 & 0 & -R7\,\psi_{L7}^{n1-1} & 0 & 0 & 0 & 0 & 0 & 0 & 0 & 0 & 0 & 0 & 0 & 1 & 0 \\
0 & 0 & 0 & 0 & 0 & 0 & 0 & -R8\,\psi_{L8}^{n1-1} & 0 & 0 & 0 & 0 & 0 & 0 & 0 & 0 & 1 & 0 & 0 & 0 \\
0 & 0 & 0 & 0 & 0 & 0 & 0 & 0 & 0 & \frac{1-i_s i_o^{-1}}{Cf} & 0 & 0 & 0 & 0 & 0 & 0 & 0 & 0 & 0 & 0 \\
0 & 0 & 0 & 0 & 0 & 0 & 0 & 0 & -\frac{1}{LF} & -\frac{RF}{LF} & 0 & 0 & 0 & 0 & 0 & 0 & 0 & 0 & 0 & 0 \\
0 & 0 & 0 & 0 & 0 & 0 & 0 & 0 & 0 & 0 & -\frac{K3}{LH1}\bar{r}_{H1}^{(m+2)} & 0 & 0 & 0 & 0 & 0 & 0 & 0 & 0 & 1 \\
0 & 0 & 0 & 0 & 0 & 0 & 0 & 0 & -1 & 0 & 0 & -\frac{K3}{LH2}\bar{r}_{H2}^{(m+2)} & 0 & 0 & 0 & 0 & 1 & 0 & 0 & 0 \\
0 & 0 & 0 & 0 & 0 & 0 & 0 & 0 & 0 & 0 & 0 & 0 & -\frac{K3}{LH3}\bar{r}_{H3}^{(m+2)} & 0 & 0 & 0 & 0 & 1 & 0 & 0 \\
0 & 0 & 0 & 0 & 0 & 0 & 0 & 0 & 0 & 0 & \frac{K3}{K2}\bar{r}_{H1}^{(m+3)}\frac{\psi_{H1}}{LH1^2} & 0 & 0 & -\frac{K1}{K2}r_{H1}^{(n-2)} & 0 & 0 & 0 & 0 & 0 & 0 \\
0 & 0 & 0 & 0 & 0 & 0 & 0 & 0 & 0 & 0 & \frac{K3}{K2}\bar{r}_{H2}^{(m+3)}\frac{\psi_{H2}}{LH2^2} & 0 & 0 & -\frac{K1}{K2}r_{H2}^{(n-2)} & 0 & 0 & 0 & 0 & 0 & 0 \\
0 & 0 & 0 & 0 & 0 & 0 & 0 & 0 & 0 & 0 & 0 & \frac{K3}{K2}\bar{r}_{H3}^{(m+3)}\frac{\psi_{H3}}{LH3^2} & 0 & 0 & -\frac{K1}{K2}r_{H3}^{(n-2)} & 0 & 0 & 0 & 0 & 0 \\
0 & \frac{1}{C1\cdot L2} & \frac{1}{C1\cdot L3} & 0 & 0 & 0 & 0 & -\frac{\psi_{L8}^{n1-1}}{C1} & 0 & 0 & 0 & -\frac{1}{C1\cdot LH2} & 0 & 0 & 0 & 0 & 0 & 0 & 0 & 0 \\
0 & 0 & 0 & \frac{1}{C2\cdot L4} & \frac{1}{C2\cdot L5} & 0 & 0 & 0 & 0 & 0 & 0 & 0 & \frac{-1}{C2\cdot LH3} & 0 & 0 & 0 & 0 & 0 & 0 & 0 \\
0 & 0 & 0 & 0 & \frac{-1}{C3\cdot L5} & \frac{1}{C3\cdot L6} & -\frac{\psi_{L7}^{n1-1}}{C3} & 0 & 0 & 0 & 0 & 0 & 0 & 0 & 0 & 0 & 0 & 0 & 0 & 0 \\
\frac{s(t)}{C4\cdot L1} & \frac{-s(t)}{C4\cdot L2} & 0 & 0 & 0 & 0 & 0 & 0 & 0 & 0 & 0 & -\frac{s(t)}{C4\cdot LH1} & 0 & 0 & 0 & 0 & 0 & 0 & 0 & 0
\end{bmatrix}$$

(A.2)

$$x = \begin{bmatrix} \psi_{L1} & \psi_{L2} & \psi_{L3} & \psi_{L4} & \psi_{L5} & \psi_{L6} & \psi_{L7} & \psi_{L8} & \upsilon_f & i_o & \psi_{H1} & \psi_{H2} & \psi_{H3} & r_{H1} & r_{H2} & r_{H3} & \upsilon_{C1} & \upsilon_{C2} & \upsilon_{C3} & \upsilon_{C4} \end{bmatrix}^T$$

$$B = \begin{bmatrix} 1 & 0 & 1 & 1 & 0 & 1 & 0 & 0 & 0 & \frac{Vdc}{Lf} & 0 & 0 & 0 & 0 & 0 & 0 & 0 & 0 & 0 & 0 \end{bmatrix}^T$$

$$u = \begin{bmatrix} \upsilon_{S1} & 0 & \upsilon_{S2} & \upsilon_{S2} & 0 & \upsilon_{S1} & 0 & 0 & 0 & U & 0 & 0 & 0 & 0 & 0 & 0 & 0 & 0 & 0 & 0 \end{bmatrix}^T$$

$$where: \quad \upsilon_{dvr} = \upsilon_f - L_T \frac{di_s}{dt}$$